Building and Environment 216 (2022) 109004

Contents lists available at ScienceDirect

Building and Environment

journal homepage: www.elsevier.com/locate/buildenv

Comparing different recalibrated methods for estimating mean radiant temperature in outdoor environment

Wanlu Ouyang [a,d], Zhixin Liu [a,*], Kevin Lau [b], Yuan Shi [c], Edward Ng [a,d,e]

[a] School of Architecture, The Chinese University of Hong Kong, New Territories, Hong Kong, China
[b] Department of Civil, Environmental and Natural Resources, Luleå Tekniska Universitet, Sweden
[c] Department of Geography & Planning, University of Liverpool, Liverpool, UK
[d] Institute of Future Cities, The Chinese University of Hong Kong, New Territories, Hong Kong, China
[e] Institute of Environment, Energy and Sustainability, The Chinese University of Hong Kong, New Territories, Hong Kong, China

ARTICLE INFO

Keywords:
Mean radiant temperature
Outdoor thermal comfort
Filed measurement
Globe thermometer
Integral radiation measurement (IRM)
Convection coefficient

ABSTRACT

Mean radiant temperature (MRT) is a significant variable for outdoor thermal comfort studies. Two measurement-based methods can estimate MRT, one is globe thermometer – cheap, easily-applied but relatively inaccurate, another is integral radiation measurement method (also known as the six-directional method) - accurate but expensive. Due to low-cost and convenience, the globe thermometer has been widely used. Previous studies have improved its estimation accuracy by recalibrating the convection coefficients in the ISO method. Thus, it is pending to cross-compare the performance of these recalibrated methods.

This study aims to investigate the transferability of the recalibrated methods for estimating MRT in outdoor environment. First, field measurement was conducted in a subtropical city, Hong Kong. MRT was obtained through two methods: globe thermometer and integral radiation method. Second, the existing recalibrated convection coefficients were summarized, and the localized convection coefficient was recalibrated. Third, all recalibrated methods were compared for their performance. The impacts of measurement locations, devices, analysis time intervals were examined.

The results showed that the newly recalibrated method achieved the lowest estimation errors (RMSE = 3.84 °C). Other recalibrated methods presented higher RMSE (3.84–17.52 °C), similar as conventional ISO method (7.91 °C). Especially for open spaces, the coefficients from other cities should be cautiously applied when the accuracy requirement is less than ±2 °C. Kestrel and Grey globe are more recommended in subtropical cities. This study shed light on the application of globe thermometer for outdoor environment, and emphasized the necessity in recalibrating the convection coefficients locally.

1. Introduction

1.1. Climate change and human biometeorology

Due to climate change, extreme weather events are increasing and intensifying [1]. Ongoing urbanization processes not only accommodate the ever-increasing population, but also lead to urban heat islands phenomenon (UHIs) [2]. Coupling the heatwaves and UHIs, the urban areas are exposed to severe and devastating heat-related mortality and morbidity [3]. Therefore, it is significant to understand the mechanisms of urban climate and identify the measures to better cope with heat stress.

Human biometeorology is a science about the interactions between the human body and atmospheric environment [4]. It involves multiple disciplinaries related to human heat stress and outdoor thermal comfort, i.e., urban climate, urban planning and design, therefore it is gaining increasing attentions in the context of urban heat islands and global warming [5]. There are two main aspects to quantify the human thermal environment: one aspect is human body characteristics – the clothing insulation, the metabolic rate, and human body parameters (age, gender, height, weight); another perspective is meteorological variables - air temperature, air velocity, humidity, and mean radiant temperature [6].

* Corresponding author.
E-mail addresses: wanlu.oy@link.cuhk.edu.hk (W. Ouyang), zhixinliu@cuhk.edu.hk (Z. Liu), kevin.lau@ltu.se (K. Lau), Yuan.Shi@liverpool.ac.uk (Y. Shi), edwardng@cuhk.edu.hk (E. Ng).

https://doi.org/10.1016/j.buildenv.2022.109004
Received 25 January 2022; Received in revised form 10 March 2022; Accepted 18 March 2022
Available online 28 March 2022

Nomenclature

MRT	Mean radiant temperature (°C)
ISO	International Organization for Standardization
IRM	Integral radiation measurement method
UHI	Urban heat island
R^2	The coefficient of determination
d	The index of agreement
MAE	Mean absolute error
MBE	Mean bias error
RMSE	Root mean square error
RMSEs	Systematic root mean square error
RMSEu	Unsystematic root mean square error
K_i	Shortwave radiation fluxes (Wm^{-2})
L_i	Longwave radiation fluxes (Wm^{-2})
W_i	The angular factor for six directions
α_k	The absorption coefficients of the clothed human body for shortwave radiations
ε_p	The absorption coefficients of the clothed human body for longwave radiations
σ	The Stefan-Bolzmann constant (= $5.67*10^{-8}$ W/m^2)
h_{cg}	The coefficient of heat transfer by convection of the globe
V_a	The wind speed (m/s)
T_g	The globe temperature (°C)
T_a	The air temperature (°C)
ε	The globe emissivity
D	The globe diameter (m)
T_i	The MRT value estimated by globe thermometer method (°C)
S_i	The MRT value estimated by integral radiation measurement method (°C)
$\overline{S}$	The mean of the MRT value estimated by integral radiation measurement method (°C)
N	Number of the data

1.2. Mean radiant temperature and measurement-based technologies for its estimation

Mean radiant temperature (MRT) is a key variable for outdoor thermal comfort, as it is decisive for the energy balance of the human body. Defined as "the uniform temperature of an imaginary enclosure in which radiant heat transfer from the human body equals the radiant heat transfer in the actual non-uniform enclosure" [7], the concept of MRT enables the investigations in the radiative exchange between human body and its surrounding environment [8]. MRT has been widely used and assessed in outdoor thermal comfort and climate-sensitive studies, i.e., calculating the outdoor thermal comfort index [9], predicting heat-related mortality [10], investigating the effect of urban geometry for heat stress [11].

Currently, there are two main measurement-based methods to estimate MRT, one is the integral radiation measurement method (IRM) and another is globe thermometer. IRM is deemed as the most accurate method to obtain MRT estimations [12], which uses pyranometer to measure the shortwave radiative fluxes and pyrgeometer to collect the longwave radiative fluxes. Afterwards, the six-directional short- and long-wave radiations are integrated with different factors following equation (1) – (2) [12,13]. Albeit the high accuracy, this method is with high costs and complexity so that is not as common as the globe thermometer method [12,14]. Globe thermometer is one of the most popular instruments in urban climate studies for MRT estimation [15]. It is based on an assumption that the radiant heat transfer depends on the surface temperature of the globe, and the convection can be estimated by air temperature and wind speed as proxies [8]. The standard globe thermometer has a diameter of 0.15 m, and is proposed for indoor environment originally. Then MRT can be estimated based on globe temperature following equation (3) – (4) [8].

$$S_{str} = \alpha_k \sum_{i=1}^{6} W_i K_i + \varepsilon_p \sum_{i=1}^{6} W_i L_i \quad (1)$$

$$MRT = \sqrt[4]{S_{str}/(\varepsilon_p \sigma)} - 273.15 \quad (2)$$

$$h_{cg} = 1.1 \times 10^8 V_a^{0.6}/D^{0.4} \quad (3)$$

$$\mathrm{MRT} = \left[(T_g + 273.15)^4 + \frac{h_{cg}}{\varepsilon} \times (T_g - T_a) \right]^{0.25} - 273.15 \quad (4)$$

Where K_i is the shortwave radiation fluxes (i = 1–6); L_i is the longwave radiation fluxes (i = 1–6); W_i is the angular factor for six directions with the sum weightings as 1, value as 0.22 for the lateral directions, and 0.06 for the up-down directions; α_k and ε_p are the absorption coefficients of the clothed human body for shortwave and longwave radiations, equal 0.7 and 0.97 respectively; σ is the Stefan-Bolzmann constant as $5.67*10^{-8}$ W/m^2; h_{cg} is the coefficient of heat transfer by convection of the globe; V_a is the wind speed (m/s); T_g is the globe temperature (°C); T_a is the air temperature (°C); ε is the globe emissivity, as 0.95 for the black globe; D is the globe diameter (unit should be m!).

1.3. Recalibration for globe thermometer

Although the globe thermometer is popular for MRT estimation, it is still questionable to be used in outdoor environments with potentially rapid changing radiant and wind conditions [16]. Three main reasons can explain the unsuitability [6]: 1) the standard globe usually takes over 20min to reach the equilibrium, which is too long for the outdoor environment with rapidly changing microclimate variables, i.e., air velocity and radiations. Therefore, the equilibrium status may not be achieved and the accuracy of the MRT estimation is uncertain; 2) the black color of the globe may absorb the shortwave radiation than expected, but it assumes both longwave and shortwave radiations are absorbed equally in the calculation of the globe thermometer; 3) the shape of the globe can be a good approximation for the seated human body, but not representative for a standing person. The spherical globe averages the radiation from all directions equally, thus may bring some estimation deviations.

Given the limitations illustrated above, some studies reduced the size of the globe to 30–50 mm, which was proved to effectively shorten the equilibrium time within 5min [12,17]. Besides, the medium grey color globe was suggested to be used, as the color is closer to the radiant properties of the skin and clothing of human beings [13,18]. As the convection coefficient h_{cg} in conventional method following equation (3) is developed for the black globe with 150 mm diameter in indoor environment. For outdoor environment, the mean convection coefficients should be recalibrated for the global thermometer with smaller size and different color [19,20].

Some researchers have recalibrated the convection coefficients of the globe thermometer for the outdoor environment in different climate backgrounds, i.e., temperate oceanic climate (*Cfb*) in Gothenburg, Sweden [12], tropical rainforest climate (*Af*) in Singapore [21–23], humid subtropical climate (*Cwa*) in Chandigarh, India [24], and hot arid climate (*Bwh*) in Tempe, Arizona [19]. These studies used the MRT values estimated by integral radiation measurement as a benchmark,

and applied non-linear regression to recalibrate the convection coefficient of the globe thermometer. Since in these studies, the sphere color (i.e., black and grey) and diameter (i.e., 38 mm, 40 mm, 50 mm, 150 mm) varied, and the background climates are different, the recalibrated convection coefficients are dissimilar (detailed values are summarized in Table 2 in the Methodology section).

1.4. Research gaps and objective

Based on the above information, three research gaps can be identified: 1) current literature recalibrated the convection coefficients in the local context, it is a pending question whether the recalibrated convection coefficients are transferable to other cities with similar or different climate backgrounds; 2) previous studies usually measure MRT and recalibrate the convection coefficients in open space, whether the coefficients can be used in other urban environments, i.e., the street canyon or tree-shaded area, is scarcely discussed so far; 3) previous studies used different thermometers to obtain Tg, it is difficult to cross-compare the impacts of the devices on the performance of different recalibrated methods. Besides, the impacts of the analysis intervals should also be explored, as the outdoor environment is featured with fast varying wind and solar conditions.

Therefore, this study aims to systematically compare the suitability of existing recalibrated methods for MRT estimation in different built environments. To achieve this aim, field measurement campaigns were firstly conducted in three sites in a subtropical city Hong Kong, i.e., open space, under tree-shading, and street canyon. Thereafter, the convection coefficient was recalibrated locally for Hong Kong. Thirdly, the MRT values were calculated based on the recalibrated methods in the previous studies and this study, and the strengths and limitations of them were assessed and compared. Besides, the impacts of measurement locations, device types, and analysis time intervals were explored and compared.

2. Methodology

The framework of the methodology in this study is presented in Fig. 1, including three steps: filed measurement, recalibrated methods, and performance comparison of the previous recalibrated and localized recalibrated methods.

2.1. Study area

Hong Kong (HK) is located on the eastern Pearl River Delta in South China, which is featured with a humid subtropical climate (*Cfa* based on Köppen-Geriger climate classification). Experiencing a long and hot summer from June to September, HK has a daily mean value of air temperature at 28.4–30.2 °C, relative humidity at 73–84%, and direct solar radiation at 6.08–16.33 MJ/m^2 during 2019–2020 [25,26]. The three measurement sites are located in the Chinese University of Hong Kong, including open space at the rooftop, street canyon between two rows of buildings in the north-south orientation, and under tree-shading near to an artificial lake. The surrounding environment of the sites and their sky view factor (SVF) were shown in Fig. 2.

2.2. Measurement scheme

The measurement campaign was taken in six partially cloudy days totally, two days for each site: Sep. 6th and Sep. 10th for the open space site, Sep. 2nd and Sep. 9th for the street canyon site, Aug. 30th and Sep. 3rd for the under tree site. On each day, the microclimate variables were collected simultaneously by stationary measurement from 9:00–17:00 (local time). Air temperature, relative humidity, wind speed, 40 mm black global temperature and 40 mm grey global temperature were measured by TESTO480, while 25.4 mm black global temperature was collected by Kestrel 5400. Besides, two sets of equipment were used to record six-directional radiations – Apogee by Apogee Instruments and CNR4 by Kipp & Zonen. All devices were set on the pedestrian height at around 1.5 m. The instrument specifications can be found in Table 1. It should be noteworthy that the globe temperature measured by Kestrel is

Table 1
Equipment specifications.

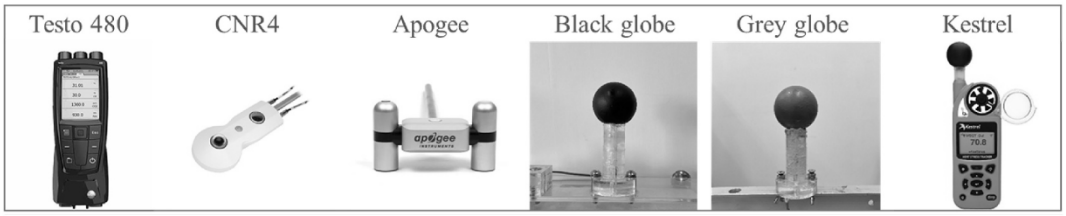

Sensors	Variable(s)	Measurement range	Accuracy	Sampling
Testo 480 Comfort level probe	Wind speed	0–5 m/s	±0.03 m/s + 4% of mv	1min
Testo 480 Temperature probe	Air temperature Relative humidity	−20 to +70 °C 0–100%	±0.2 °C ±1%	1min
Testo 480 Global thermometer 40 mm	Global temperature	0–120 °C	Class 2[a]	1min
Kestrel 5400 Heat stress tracker 1 inch	Global temperature	−29.0 to 60.0 °C	1.4 °C	1min
CNR4 Component net radiometers	Longwave and shortwave radiation in six directions	−250 to +250 W/m2 (net longwave irradiance) 0–2000 W m^{-2} (net shortwave irradiance)	**Pyrgeometer:** 5–15 μV/W/m^2 **Pyranometer:** 10–20 μV/W/m^2	1min
Apogee four-component net radiometer	Longwave and shortwave and radiation in six directions	−200 to 200 W m^{-2} (net longwave irradiance) 0–2000 W m^{-2} (net shortwave irradiance)	**Pyrgeometer:** 0.12 mV per W/m^2 **Pyranometer:** 0.057 mV per W/m^2 (upward-looking); 0.15 mV per W/m^2 (downward-looking)	1min

[a] According to standard EN 60584–2, the accuracy of Class 2 to −40 to +1200 °C (Type K).

Table 2
Standard and recalibrated methods for MRT estimation.

Source	Method name in this study	Globe thermometer	Heat convection coefficient	Limits
ISO 7726 (1998)	ISO	Black globe, 150 mm	$h_c = 1.1 * 10^8 * V_a^{0.6}/D^{0.4}$	Not specific
[12]	Thorsson	Grey globe, 38 mm	$h_c = 1.335 * 10^8 * V_a^{0.71}/D^{0.4}$	$0.1 \leq$ Va ≤ 4.0 $100 \leq$ SWin $\leq$850
[22]	Tan	Grey globe, 40 mm	$h_c = 3.42 * 10^8 * V_a^{0.119}/D^{0.4}$	$0 \leq$ Va ≤ 4.0 SWin $\leq$1300
[24]	Manavvi	Grey globe, 50 mm	$h_c = 1.5 * 10^8 * V_a^{0.93}/D^{0.4}$	$0.1 \leq$ Va ≤ 4.0 SWin $\leq$950
[16]	TeitelbaumFree	Black globe, 150 mm	$N_{ufree} = 2 + 0.589R_a^{0.25}\Big/(1 + (0.469/Pr)^{9/16})^{4/9}$ $R_a = \frac{g\beta}{\nu\alpha}(t_a - t_g)D^3$ $P_r = \frac{c_p\mu}{k}$	Free convection Pr $\geq$ 0.7 Ra $\leq$ 10^11
	TeitelbaumForce		$N_{uforce} = 2 + (0.4R_e^{0.5} + 0.06R_e^{\frac{2}{3}})P_r^{0.4}$ $R_e = \frac{v_a D}{\nu}$	Forced $0.7 \leq$ Pr ≤ 380 $0.7 \leq$ Ra ≤ 76000
	TeitelbaumMix		$Nu_{mixed} = (Nu_{free}^n + Nu_{forced}^n)^{1/n}$ $MRT = \sqrt[4]{(T_g + 273.15)^4 + \frac{Nu * k}{\varepsilon\sigma D} * (T_g - T_a)} - 273.15$	Mixed n = 4
[19]	VanosStandard	Black globe, 150 mm	$MRT_{SGT} = \sqrt[4]{(T_s + 273.15)^4 + 1.1 * 10^8 * V_a^{0.6}\Big/_{\varepsilon * D^{0.4} * (T_s - T_a)}} - 273.15$ $T_s = 1.345 * T_g - 0.369 * T_a + 0.725$	Not specific
	VanosBlack	Black globe, 40 mm	$MRT_{SGT} = \sqrt[4]{(T_s + 273.15)^4 + (0.24 + 2.08V_a^{0.5} + 1.14V_a^{0.667}) * 10^8 * (T_s - T_a)} - 273.15$ $T_s = 1.851 * T_g - 0.915 * T_a + 0.404$ for black	Not specific
	VanosGrey	Grey globe, 40 mm	$T_s = 1.6 * T_g - 0.339 * T_a - 8.69$ for grey	
[21]	Acero	Black globe, 150 mm	$h_c = 0.88 * 10^8 * V_a^{0.46}/D^{0.4}$	Not specific For clear and overcast weather
This study[a]	HKCorrect	Black globe, 40 mm Black globe, 25.4 mm (Kestrel) Grey globe, 40 mm	$h_c = 0.678 * 10^8 * V_a^{0.019}/D^{0.4}$	0.23 $\leq$ Va $\leq$3.06 m/s SWdown $\leq$1036 W m^{-2}

[a] The recalibration process and results were reported in the Result section.

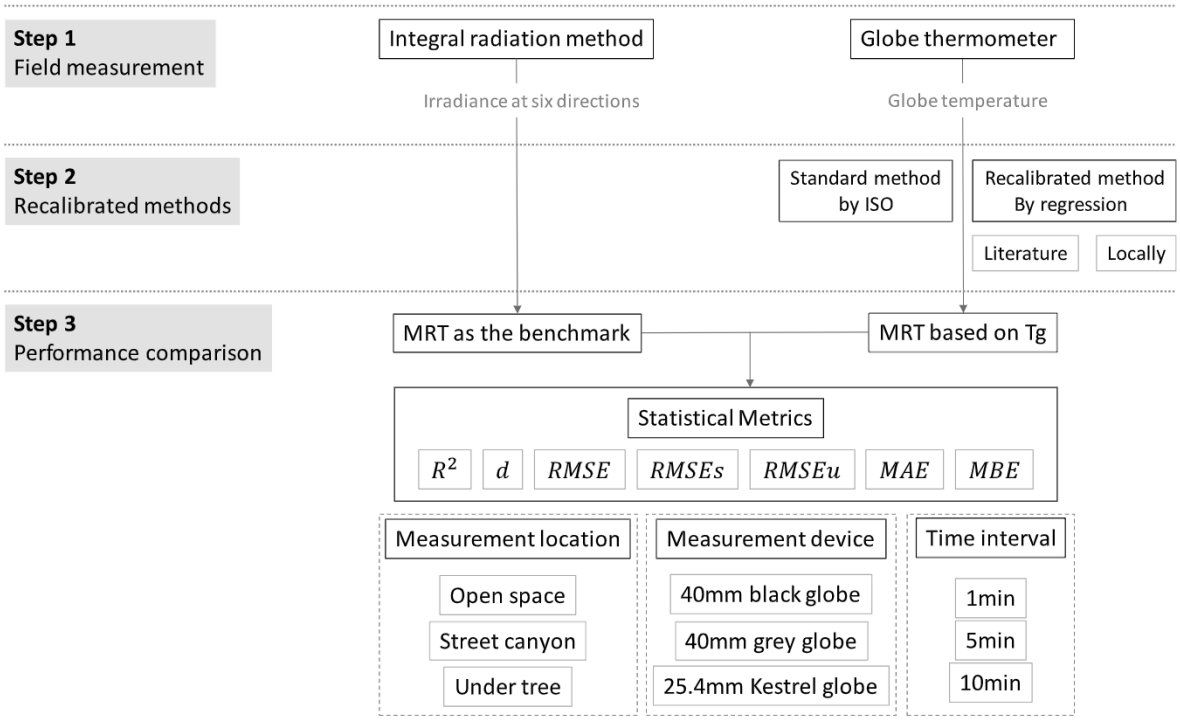

Fig. 1. Flowchart of the methodology in this study.

Fig. 2. Measurement sites and SVF.

converted to the equivalent temperature for a standard globe, thus the diameter of Kestrel globe should be 150 mm in the calculation [27].

2.3. The recalibrated methods

Current literature have recalibrated the heat convection coefficients based on the non-linear regression analysis. Using MRT values measured by integral radiation measurement as a benchmark, the best curve fit is obtained based on a higher coefficient of determination. Summarized in Table 2, these studies applied globe spheres with different diameters and colors, and were conducted in various climate backgrounds, thus the coefficients were dissimilar. Table 2 also provides a new recalibrated convection coefficient for Hong Kong, which is based on the non-linear regression results for three measurement locations and three globe devices (the details can be found in Section 3.3). Based on the listed recalibrated coefficients, the corrected values can be calculated with T_g measured by globe thermometers. Thereafter the performance of the recalibrated methods can be assessed and compared based on the MRT measured by integral radiation measurement.

2.4. The statistical metrics

Based on the recommendation of previous studies [28,29], five metrics were used to illustrate the comparison between different methods: the coefficient of determination (R^2), the root mean square error (RMSE), and its two substances - the systematic root mean square error (RMSEs) and the unsystematic root mean square error (RMSEu), the index of agreement (d), the mean bias error (MBE), and the mean absolute error (MAE). R^2 quantifies the variation between paired observations, while d indicates the ratio between the mean square error and the potential error. Both R^2 and d are dimensionless indexes, ranging from 0 to 1. RMSE describes the mean level of errors, substituted of systematic and unsystematic errors. RMSEs represents the errors existing constantly, whereas RMSEu estimates the unsystematically appearing effects. MBE denotes the average differences between paired observations, as positive value indicates overestimation and negative value implicates underestimation. MAE measures the absolute errors between paired observations. When paired observations are more similar, R^2 and d are closer to 1, RMSE and RMSEs closer to 0, RMSEu closer to RMSE, MBE and MAE closer to 0. The formulas to calculate these metrics are listed below:

$$d = 1 - \left[\sum_{i=1}^{N} (T_i - S_i)^2 \Big/ \sum_{i=1}^{N} \left(|T_i'| + |S_i'| \right)^2 \right] \tag{5}$$

$$RMSE = \left[RMSE_S^2 + RMSE_u^2 \right]^{1/2} = \left[N^{-1} \sum_{i}^{n} (T_i - S_i)^2 \right]^{1/2} \tag{6}$$

$$\text{Where : } RMSEs = \left[N^{-1} \sum_{i}^{n} (\widehat{T}_i - S_i)^2 \right]^{1/2} \tag{6a}$$

$$RMSEu = \left[N^{-1} \sum_{i}^{n} (T_i - \widehat{T}_i)^2 \right]^{1/2} \tag{6b}$$

$$MAE = N^{-1} \sum_{i}^{n} (|T_i - S_i|) \tag{7}$$

$$MBE = N^{-1} \sum_{i}^{n} (T_i - S_i) \tag{8}$$

Where $T_i' = T_i - \overline{S}$, $S_i' = S_i - \overline{S}$, and $\widehat{T}_i = a + b * S_i$; T_i is the MRT value estimated by globe thermometer; S_i represents the MRT value estimated by integral radiation measurement method; $\overline{S}$ represents the mean of the MRT value estimated by integral radiation measurement method; N denotes the number of the data;

3. Results

3.1. Measurement results

3.1.1. Integral radiation measurement and results

Previous studies usually used the MRT estimated by the integral radiation measurement (IRM) as the benchmark [16,22], as it was identified as the most accurate means to estimate MRT so far [12]. This study applied two instruments based on IRM to estimate the MRT as the

benchmark, one is the widely used CNR4 [21,22,30,31], another is recently emerging Apogee [16]. To compare the different recalibrated methods based on a solid benchmark, the reliability of the IRM was justified in this sub-section.

As shown in Fig. 3, MRT measured by CNR4 and Apogee showed a high correlation at 1-min measurement interval, all above 0.88 irrespective of measurement locations. Especially for open space, these two instruments presented nearly similar values, as the correlation coefficients were near to 1 (Fig. 3-a), and the differences of them showed random patterns (Fig. 3-b). CNR4 estimated slightly higher MRT values than Apogee in the street canyon, and presented slightly lower values under the tree. The detailed statistics of MRT estimated by CNR4 and Apogee were shown in Table 3. The deviations between these two methods were higher in the locations of open space and street canyon, as RMSE, MAE and MBE were relatively higher than the values of under tree location. One possible reason is the placement of the sensors of two methods cannot be identical, as the equipment was placed nearer to a road and a pedestrian lane for the street canyon location, and is nearer to a glass railing for the open space location (See Fig. 2). Therefore, the radiations from the surrounding may vary in the complex environment given the high sensitivity of these two instruments.

Based on the above analysis, MRT estimated by IRM was justified to be the benchmark in this study. And we applied the mean of the values of Apogee and CNR4 in the following analysis as the benchmark, thus some possible deviations related to instrument positions could be removed.

3.1.2. Globe thermometer measurement results

To test the reliability of recalibrated MRT estimation methods for different sensors, this study applied three globe thermometers to obtain the globe temperature, including 40 mm black globe, 40 mm grey globe, and 25.4 mm black globe (Kestrel). As shown in Fig. 4, globe temperature (Tg) was positively correlated with air temperature and downward shortwave radiation, regardless of thermometer types. In detail, Kestrel globe was more sensitive to the increments of air temperature and shortwave radiation due to its smaller diameter. Grey globe was more sensitive than the black one, which is reported in a previous study measured indoor [33].

Table 3
Quantitative metrics of the MRT by CNR4 vs. Apogee at 1-min time interval (*unit: °C*).

Location	R^2	d	RMSE	RMSEs	RMSEu	MAE	MBE
Under Tree	0.90	0.97	0.94	0.23	0.92	0.61	−0.05
Street Canyon	0.88	0.96	2.49	1.59	1.92	1.23	−0.79
Open Space	0.93	0.98	2.52	0.74	2.41	1.66	−0.66

3.2. Impacts of time intervals

A previous study found the analysis time interval affects the performance of MRT estimation methods in outdoor environment [12], while the time interval means taking the average at different time scales. This section investigates the impacts of time intervals, i.e., 1min, 5min, and 10min, on the performance of the ISO standard method for MRT estimation. As shown in Fig. 5, ISO method at 5min and 10min intervals yielded a better estimation result, as the scattering of the data was narrowed and correlation coefficients were improved significantly. The detailed deviations of MRT by ISO method were listed in Table 4. With increasing time intervals, the estimation biases were decreased: RMSE was reduced by 1.2–1.4 °C at 10min interval in contrast to 1min interval, while MBE was decreased by 0.2–0.3 °C.

In addition, larger time intervals effectively removed the abnormally high values of MRT, i.e., MRT above 100 °C was apparently removed by 10min interval. However, at 10min interval, the MRT values by ISO method were still abnormally high compared to the benchmark. This shows the deficiency of the standard method for its application in a subtropical climate background like HK city. Therefore, the recalibration is conducted in the next section.

3.3. Recalibrating the convection coefficient

Based on MRT by integral radiation method and microclimate variables, i.e., air temperature and wind speed, the convection coefficient of the globe can be recalibrated by non-linear regression. To obtain convection coefficient, equations (3) and (4) is transformed to be equation

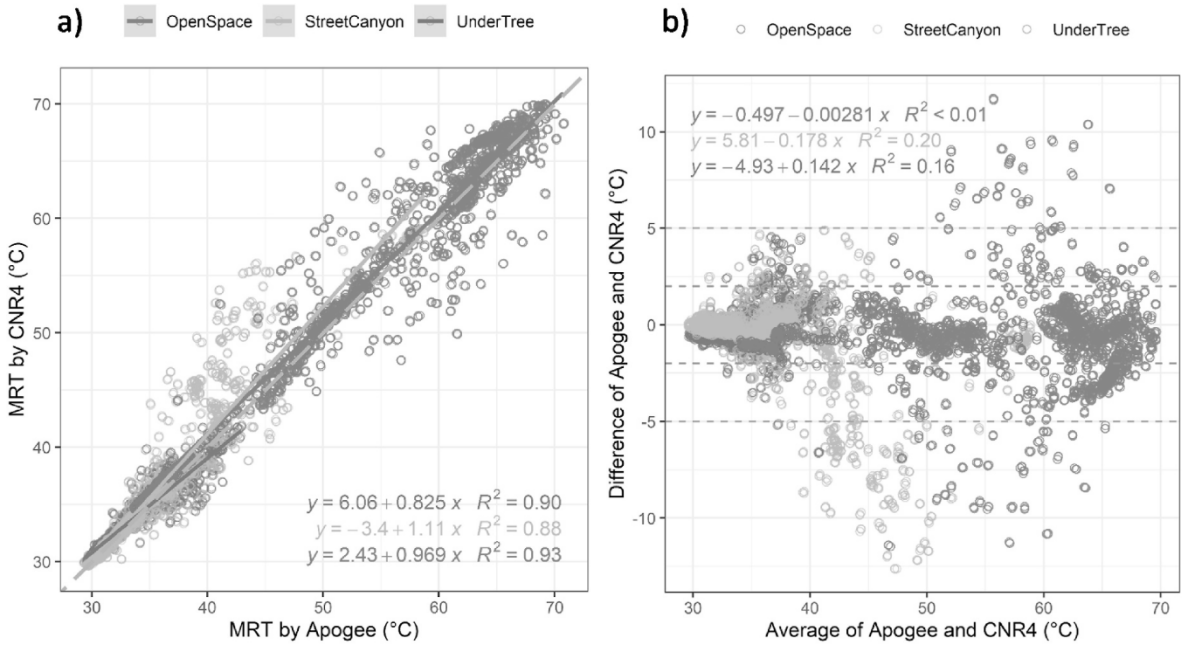

Fig. 3. Comparison between MRT by two IRM at 1min interval: a) correlation between MRT by CNR4 vs. Apogee; b) difference between MRT by CNR4 and Apogee vs. mean values of MRT by two methods. *In a), the grey dash line shows the reference line y = x; in b) the blue dash line shows the ±2 °C accuracy requirement for comfort class, and the orange dash line shows the ±5 °C accuracy requirement for stress class based on ISO standard* [32]. (For interpretation of the references to color in this figure legend, the reader is referred to the Web version of this article.)

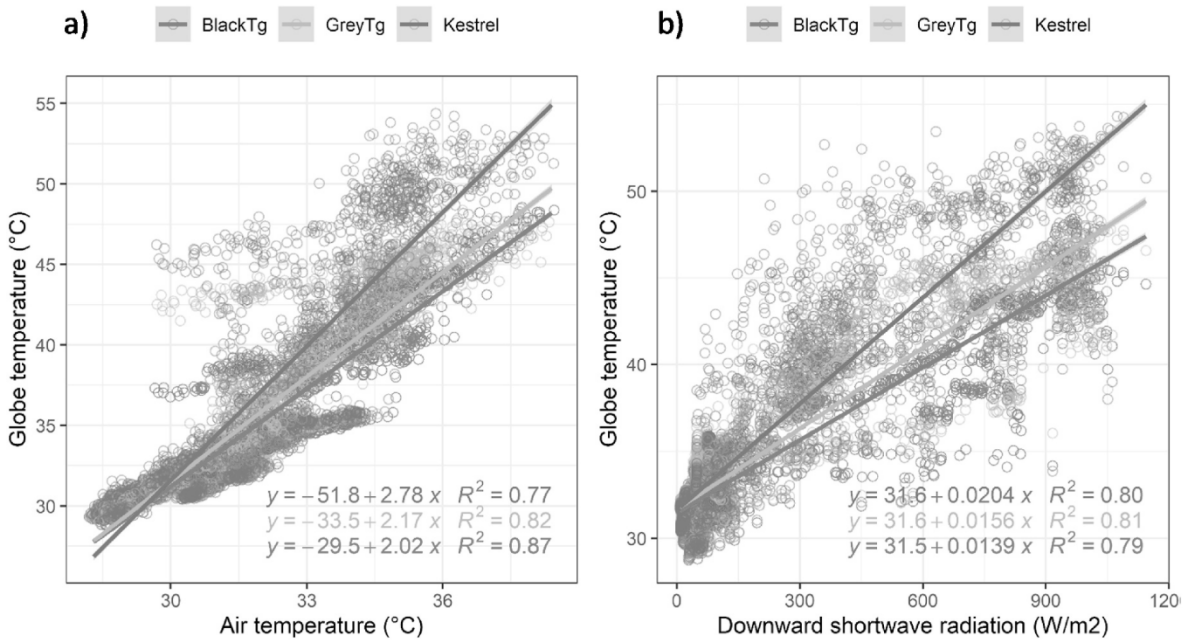

Fig. 4. Globe thermometer: a) tg vs. AT by three devices, b) Tg vs. SWdown by three devices.

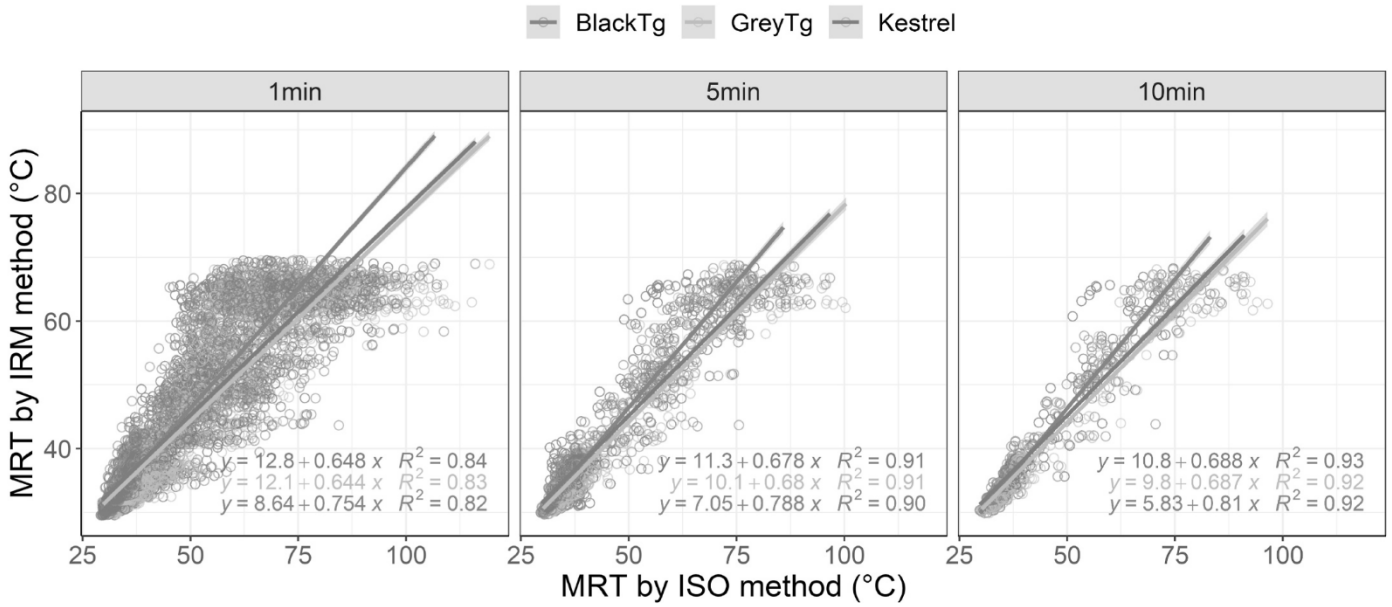

Fig. 5. MRT calculated by ISO standard coefficient and MRT measure by integral radiation method.

Table 4
Quantitative metrics of MRT estimated by Tg (ISO standard method) and by integral radiation method.

Time Interval	Device	R^2	d	RMSE	RMSEs	RMSEu	MAE	MBE
1min	Black Tg	0.82	0.93	6.67	2.73	6.09	4.25	2.50
	Grey Tg	0.83	0.90	9.20	5.89	7.06	5.63	4.81
	Kestrel	0.84	0.91	8.41	4.89	6.84	4.79	3.40
5min	Black Tg	0.90	0.96	5.51	3.00	4.61	3.80	2.53
	Grey Tg	0.91	0.92	8.27	6.50	5.11	5.30	5.16
	Kestrel	0.91	0.93	7.41	5.50	4.97	4.27	3.66
10min	Black Tg	0.92	0.96	5.06	3.26	3.88	3.41	2.80
	Grey Tg	0.92	0.92	8.04	6.57	4.63	5.22	5.18
	Kestrel	0.93	0.94	7.03	5.57	4.29	4.02	3.65

(9):

$$a * V_a^b = \frac{(MRT + 237.15)^4 - (T_g + 273.15)^4}{T_g - T_a} * \varepsilon D^4 \quad (9)$$

K-fold cross-validation is a resampling procedure to train, test, and validate the models. By splitting a given dataset into k equally-sized subsets randomly, one subset is used for testing, while the remaining subsets are used for training. After each subset is used for both training and testing, the iterations are finished and the test errors can be obtained by averaging all models' errors. Usually, it is recommended to use k = 5 or 10, considering both computational advantages and bias-variance trade-off [34]. Therefore, this study applied 5-fold cross-validation (80% as training and 20% as testing) to determine the final optimal model, which yields the convection coefficient as a = 0.676*10^8, b = 0.019 in the outdoor environment of the humid subtropical climate background, considering all measurement locations (open space, street canyon, and under tree) and time intervals (1min, 5min, and 10min). The recalibrated coefficients are valid when wind speed ranging from 0.23 to 3.06 m/s and downward shortwave radiation less than 1036 W/m^2.

3.4. Comparing different recalibrated methods for MRT estimation

3.4.1. Comparing based on error probability of two accuracy requirements

ISO standard 7726:1985 specified the requirements of the accuracy for MRT at different conditions, i.e., the measuring accuracy requirement should be ±2 °C for thermal comfort level and ±5 °C for thermal stress level [32]. To cross-compare different MRT estimation methods for their performance, the error probability was calculated by the percentage of data above the threshold of ±2 °C and ±5 °C respectively. Shown in Fig. 6, the error probability of different methods varied significantly, and the variation was also presented for different measurement locations and devices.

Regarding the differences of measurement locations, a higher error probability was presented at open space than street canyon and under tree locations. In detail, for comfort requirement at ±2 °C, in open space, the error probability was high as 76–100% (TeitelbaumForce – Tan) for all previous methods. For street canyon location, the error probability was high when applying Tan (89%), VanosBlack (61%), and VanosGrey (61%), with the lowest value for TeitelbaumForce (28%) and TeitelbaumMix (29%). In terms of under tree, high error probability was shown by Tan (96%), Manavvi (59%), and Thorsson (52%), while low values were found for TeitelbaumForce (19%) and TeitelbaumMix (25%). The localized recalibrated method (HKCorrect) outperformed

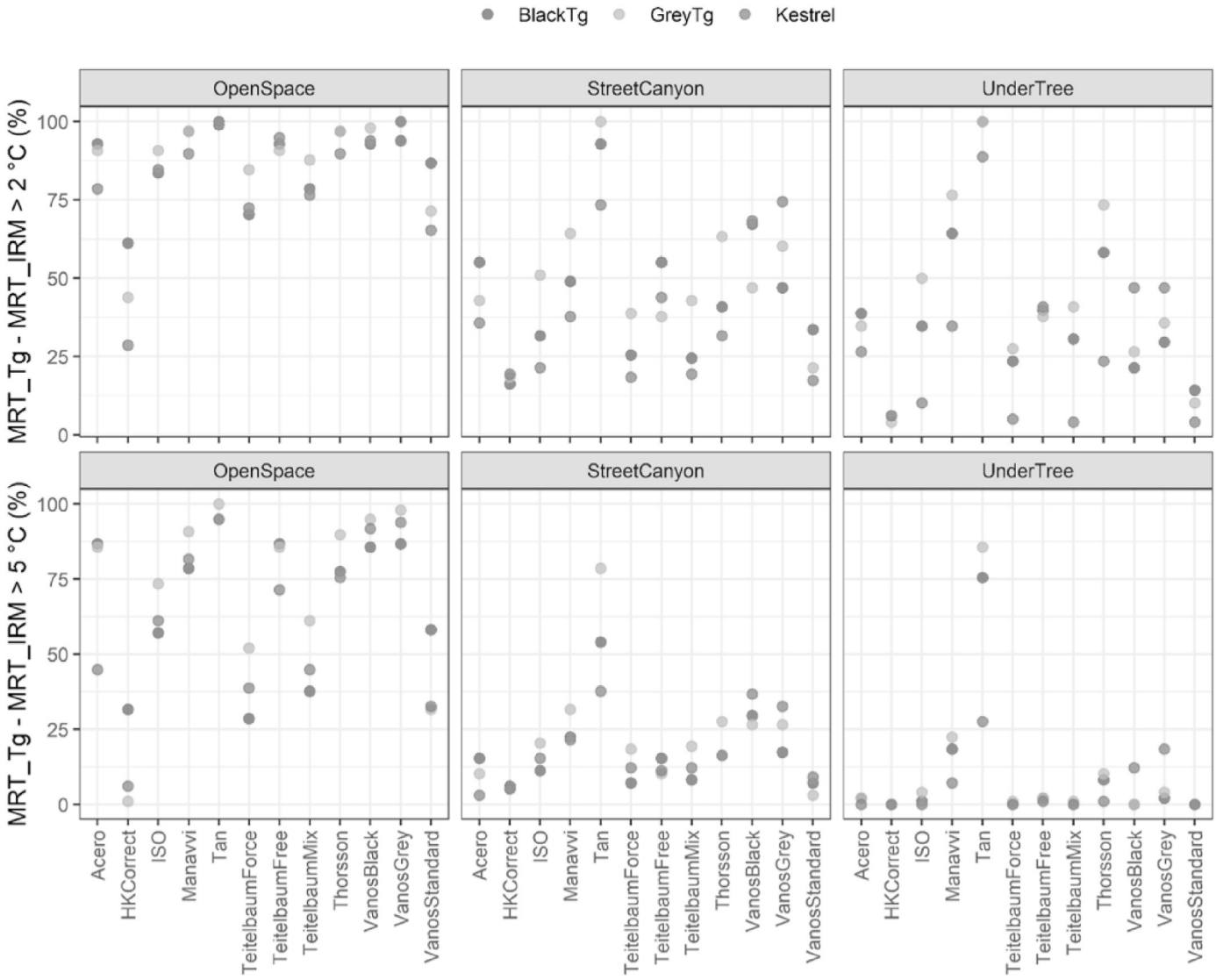

Fig. 6. Error probability (bias >2 °C and 5 °C) at 10 min interval.

with the error probability of 45%, 18%, and 5% for open space, street canyon, and under tree locations separately. For heat stress requirement at ±5 °C, at open space, all previous studies yielded the error probability of 40–97% (Teitelbaum Force – Tan). At street canyon, except the Tan (57%), VanosBlack (31%), VanosGrey (26%) methods, most of the previous studies showed the error probability lower than 25%. Under tree shading, only Tan method presented the high error probability as 63%, while TeitelbaumForce and TeitelbaumMix showed zero error probability. The localized recalibrated method (HKCorrect) still performed the best with the error probability of 13%, 5%, and 0% for open space, street canyon, and under tree locations respectively.

In terms of devices, the performance of methods was not identical. For instance, for comfort requirement at ±2 °C, grey globe showed the highest error probability among three devices for ISO (64%), Thorsson (78%), Manavvi (79%), TeitelbaymForce (50%), and TeitelbaymMix (57%), but showed the lowest value for VanosBlack (57%). Kestrel yielded the lowest error probability for ISO (39%), Thorsson (48%), Tan (87%), Manavvi (54%), TeitelbaymForce (32%), and TeitelbaymMix (33%). Similarly, for the comfort requirement at ±5 °C, grey globe also presented the highest probability for ISO (33%), Thorsson (43%), Manavvi (48%), TeitelbaymForce (24%), and TeitelbaymMix (27%). But the lowest values were attained by Kestrel for Thorsson (31%), Tan (53%), Manavvi (37%), TeitelbaymFree (28%), Acero (16%), while by black globe for ISO (23%), TeitelbaymForce (12%), TeitelbaymMix

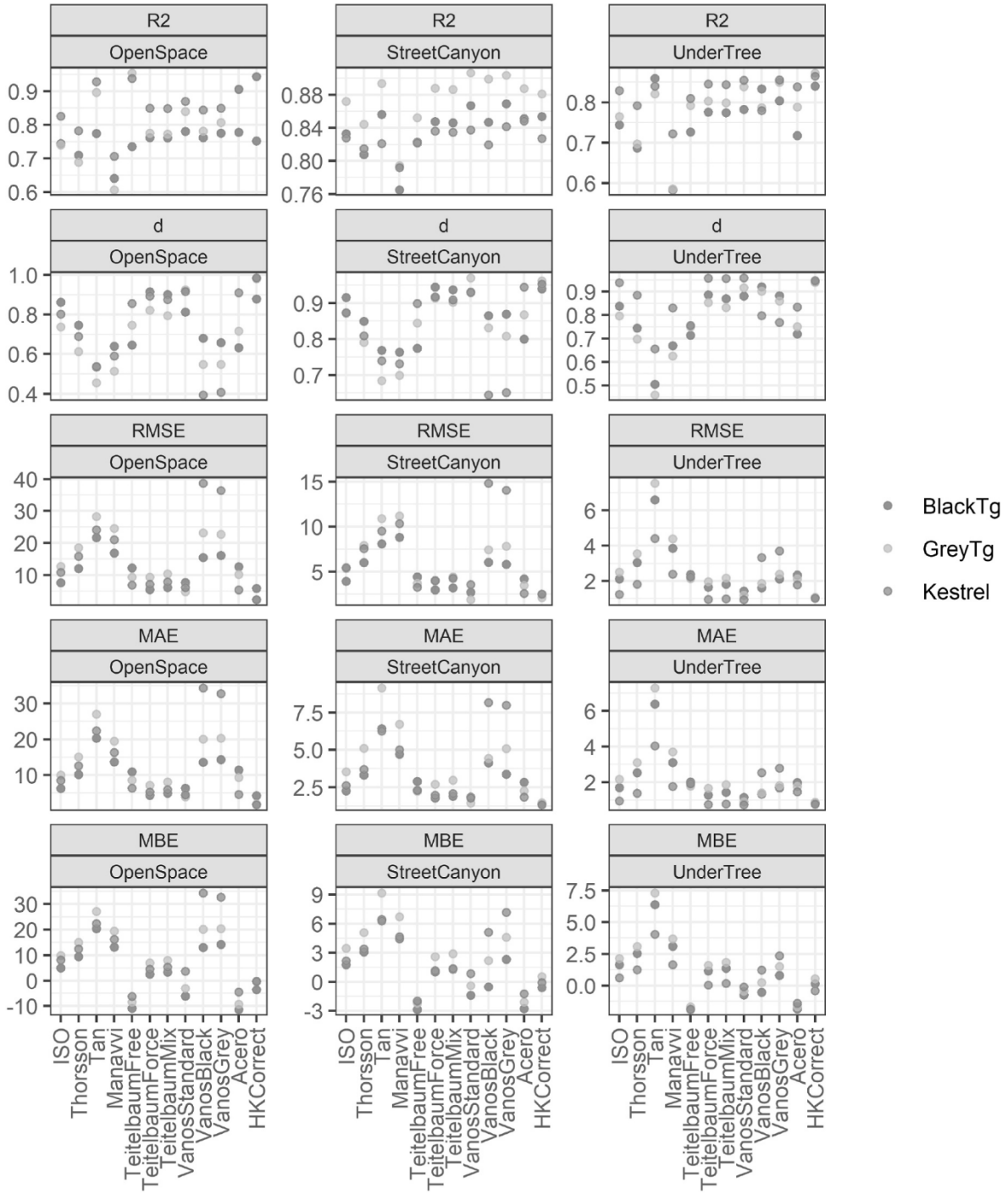

Fig. 7. Quantitative metrics of the performance of MRT estimation methods at 10min interval (*Unit of RMSE, MAE and MBE: °C*).

(15%), VanosBlack (38%), and VanosGrey (35%). Recalibrated method in HK (HKCorrect) showed the best performance among all the methods, which presented the lowest error probability, i.e., 28%, 22%, 18% for black, grey globe and Kestrel at ±2 °C requirement, and 13%, 2%, 4% at ±5 °C requirement.

3.4.2. Comparing based on quantitative metrics

The performance of different methods was quantified further by five metrics, shown in Fig. 7. Among all recalibrated methods. The localized recalibrated method (HKCorrect) exerted the best performance, with relatively high R^2 and d (R^2 = 0.84, d = 0.95), and lowest errors and biases (RMSE = 3.84 °C, MBE = −1.36 °C, MAE = 2.61 °C), while the standard ISO method yielded the results of R^2 = 0.84, d = 0.92, RMSE = 7.91 °C, MBE = 3.63 °C, MAE = 4.77 °C. The metrics for other methods were revealed in Table 5.

Regarding the impacts of the measurement locations on the accuracy of MRT estimation, the two dimensionless metrics R^2 and d showed more sensitivity to the methods than to the locations. For instance, Manavvi presented the relatively deficient performance (R^2 = 0.58–0.78, d = 0.57–0.78) in all locations, while Teitelbaum Force and Teitelbaum Mix methods showed the continuously high values regardless of locations (R^2 = 0.75–0.85 and 0.74–0.84, d = 0.87–0.92 and 0.85–0.91 respectively). Besides, Tan presented opposite performance with relatively high R^2 (0.74–0.84) but moderately low d (0.50–0.73) in all locations. As for three metrics quantifying bias and error, the values of open space were much higher than that of street canyon and under tree locations, whose differences were higher than 10 °C or even up to 20 °C. In details, some recalibrated methods yielded high errors and biases in open spaces, such as Tan method (RMSE = 24.75 °C, MBE = 23.24 °C, MAE = 23.24 °C), Manavvi (RMSE = 21.01 °C, MBE = 16.28 °C, MAE = 16.48 °C), Vanos Black (RMSE = 27.47 °C, MBE = 22.47 °C, MAE = 22.67 °C), and Vanos Grey methods (RMSE = 26.40 °C, MBE = 22.40 °C, MAE = 22.45 °C). But for street canyon and under tree location, the estimation errors and biases of these methods were reduced apparently, i.e., Tan method (RMSE = 6.33–9.55 °C, MBE = 5.90–7.27 °C, MAE = 5.90–7.28 °C), Manavvi (RMSE = 3.64–10.15 °C, MBE = 2.81–5.25 °C, MAE = 2.86–5.48 °C), Vanos Black (RMSE = 2.39–10.19 °C, MBE = 0.32–2.26 °C, MAE = 1.77–5.57 °C), and Vanos Grey methods (RMSE = 2.82–9.87 °C, MBE = 1.56–4.69 °C, MAE = 2.10–5.49 °C). This kind of difference can be partly explained by the stronger solar radiation received in the open space. The detailed differences between different locations can be found in Table A1 in the **Appendix**. Moreover, VanosStandard showed the lowest errors and biases irrespectively of the locations, with RMSE = 1.20–6.20 °C, MBE = −1.87 to −0.33 °C, MAE = 0.93–4.95 °C, which can be explained that this method was recalibrated with a standard globe. Thus the impacts of the devices should be explored further.

The results also showed that devices had effects on the accuracy of MRT estimation, as different recalibrated methods showed inconsistent patterns. For instance, the standard ISO method showed lower errors and biases for black globe with RMSE = 5.06 °C, MBE = 2.80 °C, MAE = 3.41 °C, compared with RMSE = 7.03–8.04 °C, MBE = 3.65–5.18 °C, MAE = 4.02–5.22 °C for grey globe and Kestrel. Although Thorsson et al. suggest using grey globe thermometer [12], the comparison showed that Thorsson method presented lower errors and bias based on black globe than that of grey globe: RMSE = 7.94 vs. 11.77 °C, MBE = 5.01 vs. 7.74 °C, MAE = 5.35 vs. 7.75 °C. In terms of the localized recalibrated method, HKCorrect reached the lowest estimation errors and biases for grey globe (RMSE = 1.91 °C, MBE = 0.28 °C, MAE = 1.43 °C) than Kestrel and black globe (RMSE = 2.03–3.70 °C, MBE = −1.35 to −0.25 °C, MAE = 1.25–2.14 °C). Other details regarding different devices were reported in Table A2 in the **Appendix**.

4. Discussion

4.1. Recalibration and transferability of methods

Previous studies recalibrated the convection coefficients when estimating MRT based on Tg, because the conventional method for MRT estimation is developed for the standard environmental conditions, i.e., low wind speed (<0.15 m/s) and moderate temperature (= 20 °C) [8], thus they may not be applicable for outdoor environment in different climate backgrounds [6]. Summarized in Table 2, the recalibrated coefficients are various for different climate types with various wind and solar conditions.

To investigate the transferability of the recalibrated coefficients to other cities, this study cross-compared the performance of different convection coefficients in a subtropical climate background. Three measurement locations and three types of globe thermometers were involved for the comparison. The results showed the recalibrated coefficients performed inconsistently, some coefficients were inferior to others, especially for open space. Besides, even though with similar climate background, the transferability is not definitely feasible. For instance, Singapore is in a similar hot and humid as well as high solar radiation with HK, yet the method developed by Tan [22,23] was not applicable in HK with high errors and biases (RMSE = 15.86 °C, MBE = 12.04 °C, MAE = 12.07 °C). India is in the same humid subtropical (*Cfa*) climate with HK, the method developed by Manavvi [24] was also with large deviations from the benchmark by the integral radiation method (RMSE = 15.74 °C, MBE = 7.94 °C, MAE = 8.96 °C). Another method conducted in Singapore by Acero [21] showed relatively lower errors and biases, but still much above ±2 °C (RMSE = 6.57 °C, MBE = −4.17 °C, MAE = 4.42 °C). These results indicate the transferability of the recalibrated methods is limited, which can be partially explained that radiant environment and wind velocity vary largely. Therefore, the results in this study signify the necessity to recalibrate the convection coefficients when estimating MRT with Tg when the accuracy requirement is high up to ±2 °C.

4.2. Recalibration and convection process

There are two types of errors and biases, one is between the globe

Table 5
Quantitative metrics of different MRT estimation methods.

Methods	R^2	d	RMSE	RMSEs	RMSEu	MAE	MBE
ISO	0.84	0.92	7.91	4.58	6.45	4.77	3.63
Thorsson	0.80	0.86	11.38	7.63	8.44	6.77	5.88
Tan	0.92	0.80	15.86	14.69	5.98	12.07	12.04
Manavvi	0.72	0.79	15.74	10.55	11.69	8.96	7.94
TeitelbaumFree	0.91	0.90	6.41	5.93	2.43	4.46	−4.30
TeitelbaumForce	0.86	0.95	5.96	2.65	5.34	3.65	2.20
TeitelbaumMix	0.86	0.94	6.41	3.26	5.52	3.92	2.67
VanosStandard	0.85	0.96	4.87	1.57	4.61	3.03	−1.00
VanosBlack	0.82	0.78	17.52	13.85	10.73	10.08	8.16
VanosGrey	0.84	0.79	16.84	13.75	9.72	9.97	9.30
Acero	0.87	0.90	6.57	5.84	3.00	4.42	−4.17
HKCorrect	**0.84**	**0.95**	**3.84**	**1.97**	**3.29**	**2.61**	**−1.36**

thermometer and the integral radiation method, another is between the different estimation methods based on the globe thermometer. The former type is partly explained by the shape of the standing men, as the globe thermometer is based on the sphere while the integral radiation method is based on the cuboid shape [35]. Besides, the globe thermometer is an indirect way to derive MRT by determining the energy balance of a measuring system, while the integral radiation method is an active method to measure the shortwave and longwave radiant fluxes in six directions to represent a human body [36]. Therefore, the integral radiation method has been identified to be the most accurate so far for MRT estimation [12], and used as the benchmark to compare the different calibrated coefficients.

As for the errors and biases between the different convection coefficients, there are two possible explanations. One is based on the characteristics of the globe, the emissivity of the globe is varied based on the coating color [8], thus the deviations of black and grey globes are different given the results in this study. Another main reason is the different climate background, i.e, the wind speed and solar radiation conditions, which affect the convection processes of the globe. The recalibration is emphasized for localized application, since the convection process varies due to the different climate backgrounds. The varying coefficients can be explained by the assumption of the globe thermometer, which refers to the balance of the thermal exchanges between the globe and the microclimate environment [8]. This balance is achieved by convection, in which the heat transferring between the air inside the globe and its surrounding environment. There are mainly two types of convection: free convection and forced convection [16]. Previous studies indicate that free convection is dominant when the wind speed is low, i.e., lower than 0.2 m/s in Ref. [16], while forced convection becomes more importantly with increasing wind speed compared to free convection. This means for outdoor studies using 40 mm diameter globe, forced convection plays a dominating role [19]. Therefore, mixed convection is suggested to be considered for MRT estimation [19]. Our study confirmed this finding by comparing the recalibrated methods based on the free, forced and mixed convection processes, and the results showed when applying in a subtropical climate city, like Hong Kong, the TeitelbaumForce and TeitelbaumMix methods showed slightly higher fits (R^2 = 0.86, d = 0.94–0.95) and slightly lower biases (RMSE = 5.96–6.41 °C, MBE = 2.20–2.67 °C, MAE = 3.65–3.92 °C) than TeitelbaumFree method ((R^2 = 0.91, d = 0.90, RMSE = 6.41 °C, MBE = −4.30 °C, MAE = 4.46 °C).

4.3. Impacts of time intervals

The convection balance of the globe thermometer is also affected by the analysis time intervals, as the outdoor environment is featured with a fast-varying wind and radiative condition. This study compared three time intervals: 1min, 5min, and 10min for their impacts on the MRT estimation. The results in this study were consistent with the findings in the previous study that a larger interval can smooth the deviations of the wind, radiation, and temperature, so that the MRT estimation is more realistic compared to the benchmark [12,16,21]. Therefore, 10min time interval is used and suggested in our study when estimating MRT in outdoor environment based on Tg, which was also recommended by Ref. [37].

4.4. Significance and implications

This study, to our knowledge, is the first study to systematically compare the MRT estimation methods based on Tg. It contributes to the urban climate and outdoor thermal comfort studies in two aspects: 1) for studies in a subtropical climate city in HK, this study provides a new recalibrated coefficient for MRT estimation, so that the MRT can be estimated through the cheap and convenient method (globe thermometer) and with relatively high accuracy; 2) for studies in other cities, this study implies that it should be cautious to use ISO standard method to estimate MRT, or directly apply the recalibrated coefficients in different cities, especially when the requirement of the accuracy for MRT is high as ±2 °C for thermal comfort level [32].

4.5. Limitations and further studies

The limitations are discussed for a better understanding in this study and for inspiring the future studies. Firstly, this study only focused on the typical summer days in Hong Kong, and compared the sites with different SVFs. This is because the heat stress is severe in the summer period as solar radiation is dominant for energy fluxes, and the typical summer day is the most frequent in Hong Kong [38]. Thus, this study proved that the newly recalibrated coefficients are valid in the summer season in partially cloudy weather conditions. Its feasibility in other meteorological conditions and seasons should be tested in the following studies. Secondly, this study focused on comparing the applicability of different MRT estimation methods and their performance in different sites and by different measurement devices, thus it only covers the three types of urban morphology types, namely open space, street canyon, and under tree. However, there are other morphological characteristics, i.e., building height, building density, and aspect ratio, whose impacts on the convection process of globe thermometer is a possible direction to explore. Thirdly, the ellipsoid shaped sensor can have a close approximation the human shapes regardless of the standing or seated status [8], thus its usage can be expected in the future studies.

5. Conclusions

Mean radiant temperature (MRT), as one of the most significant microclimate variables, has been widely estimated by globe thermometers in outdoor thermal comfort studies. To improve the accuracy of MRT estimation, recalibrated methods have been proposed and applied in different cities. It is worth exploring whether these recalibrated methods can be transferred to other cities. Inspired by this pending question, this study applied MRT by the integral radiation method (also known as six-directional method) as the benchmark, and compared the performance of different recalibrated methods for estimating MRT based on thermometer temperature in a subtropical climate city, Hong Kong. The convection coefficient was recalibrated through non-linear regression analysis for MRT estimation based on Tg, and joined in the performance comparison. Besides, the impacts of measurement locations, thermometer types, and analysis time intervals were also investigated. The findings of this study can be summarized in the following aspects:

1) For the performance of different methods, the ISO standard method and recalibrated methods in different cities should be carefully used in the open space in a subtropical climate. Especially for accuracy requirement at ±2 °C, it is suggested to take a local recalibration for the convection coefficient instead of directly using the formula in the literature.
2) For different globe thermometers, Kestrel and Grey globe are more recommended in the outdoor environment in the subtropical climate background, as they presented higher fits, lower errors and biases in contrast to the benchmark. Black globe can be applied when the accuracy requirement is ±5 °C.
3) For analysis time intervals, 1min interval is not recommended when estimating MRT based on Tg in the outdoor environment, as the varying wind and solar conditions may bring many uncertainties for the results. This study suggests applying 10min as the analysis interval, 5min is also appropriate when the wind and solar conditions are stable.

This study indicates that thermometer devices can be used in outdoor environment, but the convection coefficient should be recalibrated carefully. The coefficients in the previous studies may be transferable in the street canyon or tree-shaded areas with an accuracy requirement at

±5 °C, but should not be applied in the open space with an accuracy requirement at ±2 °C. The findings of this study contribute to improving the MRT measurement accuracy based on cheap methods.

CRediT authorship contribution statement

Wanlu Ouyang: Writing – review & editing, Writing – original draft, Visualization, Methodology, Formal analysis, Conceptualization. **Zhixin Liu:** Data curation, Project administration, Writing – review & editing. **Kevin Lau:** Writing – review & editing, Methodology. **Yuan Shi:** Methodology, Writing – review & editing. **Edward Ng:** Supervision, Project administration, Funding acquisition.

Declaration of competing interest

The authors declare that they have no known competing financial interests or personal relationships that could have appeared to influence the work reported in this paper.

Acknowledgment

This research is supported by the General Research Fund (RGC Ref No. 14617220) from the Research Grants Council (RGC) of Hong Kong. The authors also want to thank the student helpers Mr. Donghang Qi and Mr. Kam Ming Ng for their help with the field measurements.

Appendix A

Table A1
Quantitative metrics of different MRT estimation methods for three locations at 10 min interval

Location	MRT methods	R^2	d	RMSE	RMSEs	RMSEu	MAE	MBE
Open Space	ISO	0.74	0.79	10.54	8.09	6.75	8.24	7.70
	Thorsson	0.70	0.67	15.63	13.01	8.66	12.59	12.28
	Tan	0.84	0.50	24.75	23.90	6.46	23.24	23.24
	Manavvi	0.63	0.57	21.01	17.44	11.70	16.48	16.28
	TeitelbaumFree	0.79	0.74	9.67	9.20	2.99	8.61	−8.59
	TeitelbaumForce	0.77	0.87	7.47	4.85	5.67	5.58	4.67
	TeitelbaumMix	0.77	0.85	8.27	5.84	5.87	6.33	5.60
	VanosStandard	0.66	0.89	6.26	2.03	5.92	4.95	−1.87
	VanosBlack	0.64	0.48	27.47	24.07	13.24	22.67	22.47
	VanosGrey	0.67	0.49	26.40	23.65	11.72	22.45	22.40
	Acero	0.69	0.74	9.84	9.02	3.93	8.47	−8.45
	HKCorrect	**0.84**	**0.95**	**3.84**	**1.97**	**3.29**	**2.61**	**−1.36**
Street Canyon	ISO	0.83	0.88	4.96	3.38	3.63	2.80	2.46
	Thorsson	0.81	0.81	7.21	5.51	4.66	4.04	3.86
	Tan	0.84	0.73	9.55	8.45	4.45	7.28	7.27
	Manavvi	0.78	0.73	10.15	7.96	6.31	5.48	5.25
	TeitelbaumFree	0.80	0.84	3.82	3.45	1.64	2.48	−2.36
	TeitelbaumForce	0.85	0.92	3.70	2.09	3.05	2.15	1.60
	TeitelbaumMix	0.84	0.91	4.00	2.44	3.17	2.32	1.86
	VanosStandard	0.79	0.94	2.80	0.51	2.75	1.69	−0.33
	VanosBlack	0.78	0.74	10.19	7.52	6.88	5.57	2.26
	VanosGrey	0.81	0.74	9.87	7.87	5.95	5.49	4.69
	Acero	0.80	0.88	3.48	2.94	1.86	2.31	−2.06
	HKCorrect	**0.83**	**0.95**	**2.37**	**1.04**	**2.13**	**1.38**	**−0.05**
Under Tree	ISO	0.74	0.85	2.03	1.48	1.39	1.61	1.47
	Thorsson	0.68	0.76	2.90	2.29	1.77	2.35	2.29
	Tan	0.74	0.52	6.33	5.99	2.04	5.90	5.90
	Manavvi	0.59	0.69	3.64	2.83	2.29	2.86	2.81
	TeitelbaumFree	0.77	0.74	2.25	2.13	0.72	1.92	−1.82
	TeitelbaumForce	0.75	0.90	1.58	0.98	1.23	1.24	0.94
	TeitelbaumMix	0.74	0.88	1.73	1.15	1.29	1.37	1.13
	VanosStandard	0.80	0.92	1.20	0.83	0.86	0.93	−0.43
	VanosBlack	0.75	0.86	2.39	1.19	2.08	1.77	0.32
	VanosGrey	0.81	0.83	2.82	2.10	1.88	2.10	1.56
	Acero	0.77	0.77	2.09	1.95	0.75	1.75	−1.64
	HKCorrect	**0.82**	**0.94**	**1.04**	**0.61**	**0.84**	**0.83**	**0.09**

Table A2
Quantitative metrics of different MRT estimation methods for three devices at 10 min interval

Device	MRT methods	R2	d	RMSE	RMSEs	RMSEu	MAE	MBE
BlackTg	ISO	0.92	0.96	5.06	3.26	3.88	3.41	2.80
	Thorsson	0.91	0.92	7.94	6.19	4.98	5.35	5.01
	Tan	0.94	0.82	13.84	13.01	4.72	11.04	11.04
	Manavvi	0.87	0.87	11.19	8.86	6.82	7.15	6.89
	TeitelbaumFree	0.93	0.85	7.58	7.35	1.86	5.28	−5.24
	TeitelbaumForce	0.93	0.98	3.72	1.65	3.33	2.46	1.56
	TeitelbaumMix	0.93	0.97	4.10	2.22	3.45	2.76	2.02
	VanosStandard	0.94	0.95	4.74	4.21	2.17	3.12	−2.80
	VanosBlack	0.93	0.91	9.61	8.14	5.12	6.35	3.98
	VanosGrey	0.94	0.90	9.95	8.77	4.69	6.46	5.76

(*continued on next page*)

Table A2 (*continued*)

Device	MRT methods	R2	d	RMSE	RMSEs	RMSEu	MAE	MBE
	Acero	0.94	0.84	7.78	7.61	1.64	5.43	−5.37
	HKCorrect	**0.94**	**0.97**	**3.70**	**2.77**	**2.44**	**2.14**	**−1.35**
GreyTg	ISO	0.92	0.92	8.04	6.57	4.63	5.22	5.18
	Thorsson	0.90	0.86	11.77	10.03	6.16	7.75	7.74
	Tan	0.97	0.76	18.00	17.56	3.94	14.50	14.50
	Manavvi	0.85	0.80	15.77	13.20	8.63	9.97	9.95
	TeitelbaumFree	0.98	0.91	5.91	5.78	1.24	4.21	−4.15
	TeitelbaumForce	0.94	0.95	5.99	4.61	3.82	3.84	3.74
	TeitelbaumMix	0.93	0.94	6.62	5.30	3.96	4.32	4.27
	VanosStandard	0.96	0.98	3.03	2.09	2.19	2.11	−1.32
	VanosBlack	0.94	0.84	14.04	12.84	5.68	8.64	7.51
	VanosGrey	0.95	0.84	13.89	12.95	5.00	9.07	8.80
	Acero	0.97	0.90	6.31	6.17	1.34	4.46	−4.37
	HKCorrect	**0.98**	**0.99**	**1.91**	**0.92**	**1.67**	**1.43**	**0.28**
Kestrel	ISO	0.93	0.94	7.03	5.57	4.29	4.02	3.65
	Thorsson	0.91	0.89	10.15	8.48	5.56	5.88	5.69
	Tan	0.97	0.82	15.12	14.55	4.09	10.88	10.87
	Manavvi	0.88	0.84	13.56	11.21	7.62	7.70	7.49
	TeitelbaumFree	0.97	0.96	4.55	4.24	1.65	3.52	−3.39
	TeitelbaumForce	0.94	0.97	4.71	3.13	3.52	2.67	1.91
	TeitelbaumMix	0.94	0.96	5.18	3.68	3.64	2.94	2.31
	VanosStandard	0.95	0.98	4.10	2.56	3.20	2.34	1.49
	VanosBlack	0.94	0.71	23.98	22.67	7.82	15.02	13.56
	VanosGrey	0.94	0.72	22.59	21.52	6.87	14.51	14.08
	Acero	0.96	0.97	3.59	3.00	1.97	2.65	−2.42
	HKCorrect	**0.97**	**0.99**	**2.02**	**0.26**	**2.01**	**1.25**	**−0.25**

References

[1] IPCC, Summary for policymakers, in: Climate Change 2021: the Physical Science Basis. Contribution of Working Group I to the Sixth Assessment Report of the Intergovernmental Panel on Climate Change, 2021.

[2] T.R. Oke, The energetic basis of the urban heat island, Q. J. R. Meteorol. Soc. 108 (455) (1982) 1–24.

[3] D. Wang, K.K.-L. Lau, C. Ren, W.B.I. Goggins, Y. Shi, H.C. Ho, T.-C. Lee, L.-S. Lee, J. Woo, E. Ng, The impact of extremely hot weather events on all-cause mortality in a highly urbanized and densely populated subtropical city: a 10-year time-series study (2006-2015), Sci. Total Environ. 690 (2019) 923–931, https://doi.org/10.1016/j.scitotenv.2019.07.039.

[4] P. Höppe, Aspects of human biometerology in past, present and future, Int. J. Biometeorol. 40 (1) (1997) 19–23, https://doi.org/10.1007/BF02439406.

[5] G.R. McGregor, Human biometeorology, Prog. Phys. Geogr.: Earth Environ. 36 (1) (2012) 93–109, https://doi.org/10.1177/0309133311417942.

[6] N. Kántor, A. Kovács, T.-P. Lin, Looking for simple correction functions between the mean radiant temperature from the "standard black globe" and the "six-directional" techniques in Taiwan, Theor. Appl. Climatol. 121 (1) (2015) 99–111, https://doi.org/10.1007/s00704-014-1211-2.

[7] ASHRAE, 2001 ASHRAE Handbook: Fundamentals, American Society of Heating, Refrigerating and Air-Conditioning Engineers, 2001. https://books.google.com.hk/books?id=k9qeAQAACAAJ.

[8] ISO, BS EN ISO 7726:2001-Ergonomics of the thermal environment, in: Instruments for measuring physical quantities, 2001. https://www.standardsuk.com/products/BS-EN-ISO-7726-2001.

[9] H. Guo, D. Aviv, M. Loyola, E. Teitelbaum, N. Houchois, F. Meggers, On the understanding of the mean radiant temperature within both the indoor and outdoor environment, a critical review, Renew. Sustain. Energy Rev. 117 (2020), 109207, https://doi.org/10.1016/j.rser.2019.06.014.

[10] S. Thorsson, J. Rocklöv, J. Konarska, F. Lindberg, B. Holmer, B. Dousset, D. Rayner, Mean radiant temperature - a predictor of heat related mortality, Urban Clim. 10 (2014) 332–345, https://doi.org/10.1016/j.uclim.2014.01.004.

[11] K.K.-L. Lau, F. Lindberg, D. Rayner, S. Thorsson, The effect of urban geometry on mean radiant temperature under future climate change: a study of three European cities, Int. J. Biometeorol. 59 (7) (2015) 799–814, https://doi.org/10.1007/s00484-014-0898-1.

[12] S. Thorsson, F. Lindberg, I. Eliasson, B. Holmer, Different methods for estimating the mean radiant temperature in an outdoor urban setting, Int. J. Climatol. 27 (14) (2007) 1983–1993, https://doi.org/10.1002/joc.1537.

[13] N. Kántor, J. Unger, The most problematic variable in the course of human-biometeorological comfort assessment-The mean radiant temperature, Cent. Eur. J. Geosci. 3 (1) (2011) 90–100, https://doi.org/10.2478/s13533-011-0010-x.

[14] H. Lee, S. Jo, S. Park, A simple technique for the traditional method to estimate mean radiant temperature, Int. J. Biometeorol. (2021), https://doi.org/10.1007/s00484-021-02213-x.

[15] E. Johansson, S. Thorsson, R. Emmanuel, E. Krüger, Instruments and methods in outdoor thermal comfort studies - the need for standardization, Urban Clim. 10 (2014) 346–366, https://doi.org/10.1016/j.uclim.2013.12.002.

[16] E. Teitelbaum, K.W. Chen, F. Meggers, H. Guo, N. Houchois, J. Pantelic, A. Rysanek, Globe thermometer free convection error potentials, Sci. Rep. 10 (1) (2020) 2652, https://doi.org/10.1038/s41598-020-59441-1.

[17] M. Nikolopoulou, N. Baker, K. Steemers, Improvements to the globe thermometer for outdoor use, Architect. Sci. Rev. 42 (1) (1999) 27–34, https://doi.org/10.1080/00038628.1999.9696845.

[18] ISO, ISO 7726:1998 (E)-Ergonomics of the Thermal Environment-Instruments for Measuring Physical Quantities, 1998.

[19] J.K. Vanos, K. Rykaczewski, A. Middel, D.J. Vecellio, R.D. Brown, T.J. Gillespie, Improved methods for estimating mean radiant temperature in hot and sunny outdoor settings, Int. J. Biometeorol. 65 (6) (2021) 967–983, https://doi.org/10.1007/s00484-021-02131-y.

[20] S. Wang, Y. Li, Suitability of acrylic and copper globe thermometers for diurnal outdoor settings, Build. Environ. 89 (2015) 279–294, https://doi.org/10.1016/j.buildenv.2015.03.002.

[21] J.A. Acero, A. Dissegna, Y.S. Tan, A. Tan, L.K. Norford, A. Ruefenacht, E.J.Y. Koh, Y.S. Tan, L.K. Norford, Outdoor performance of the black globe temperature sensor on a hot and humid tropical region, Environ. Technol. (ja) (2021) 1–20, https://doi.org/10.1080/09593330.2021.1989057, 0.

[22] C.L. Tan, N.H. Wong, S.K. Jusuf, Outdoor mean radiant temperature estimation in the tropical urban environment, Build. Environ. 64 (2013) 118–129, https://doi.org/10.1016/j.buildenv.2013.03.012.

[23] C.L. Tan, N.H. Wong, P.Y. Tan, S.K. Jusuf, Z.Q. Chiam, Impact of plant evapotranspiration rate and shrub albedo on temperature reduction in the tropical outdoor environment, Build. Environ. 94 (2015) 206–217, https://doi.org/10.1016/j.buildenv.2015.08.001.

[24] S. Manavvi, E. Rajasekar, Estimating outdoor mean radiant temperature in a humid subtropical climate, Build. Environ. 171 (2020), 106658, https://doi.org/10.1016/j.buildenv.2020.106658.

[25] HKO, Summary of Meteorological and Tidal Observations in Hong Kong, 2019.

[26] HKO, Summary of meteorological and tidal observations in Hong Kong. https://www.hko.gov.hk/tc/publica/smo/files/SMO2020.pdf, 2020.

[27] Kestrel Instruments, User guide of Kestrel 5400 heat stress tracker. https://kestrelinstruments.com/mwdownloads/download/link/id/14/, 2021.

[28] C.J. Willmott, On the validation of models, Phys. Geogr. 2 (2) (1981) 184–194, https://doi.org/10.1080/02723646.1981.10642213.

[29] C.J. Willmott, Some comments on the evaluation of model performance, Bull. Am. Meteorol. Soc. 63 (11) (1982) 1309–1313. https://doi.org/10.1175/1520-0477(1982)063<1309:SCOTEO>2.0.CO;2.

[30] A. Lai, M. Maing, E. Ng, Observational studies of mean radiant temperature across different outdoor spaces under shaded conditions in densely built environment, Build. Environ. 114 (2017) 397–409, https://doi.org/10.1016/j.buildenv.2016.12.034.

[31] W. Ouyang, T.E. Morakinyo, C. Ren, S. Liu, E. Ng, Thermal-irradiant performance of green infrastructure typologies: field measurement study in a subtropical climate city, Sci. Total Environ. 764 (2021), 144635, https://doi.org/10.1016/j.scitotenv.2020.144635.

[32] ISO, BS EN ISO 27726:1994-Thermal Environments-Instruments and Methods for Measuring Physical Quantities, 1985.

[33] N. Walikewitz, B. Jänicke, M. Langner, F. Meier, W. Endlicher, The difference between the mean radiant temperature and the air temperature within indoor environments: a case study during summer conditions, Build. Environ. 84 (2015) 151–161, https://doi.org/10.1016/j.buildenv.2014.11.004.

[34] G. James, D. Witten, T. Hastie, R. Tibshirani, An Introduction to Statistical Learning, vol. 112, Springer, 2013.

[35] R.D. Brown, Correcting the error in measuring radiation received by a person: introducing cylindrical radiometers, Sensors 19 (23) (2019) 5085, https://doi.org/10.3390/s19235085.

[36] H. Staiger, A. Matzarakis, Accuracy of mean radiant temperature derived from active and passive radiometry, Atmosphere 11 (8) (2020) 805, https://doi.org/10.3390/atmos11080805.

[37] C. Marino, A. Nucara, M. Pietrafesa, E. Polimeni, S. Costanzo, Outdoor mean radiant temperature estimation: is the black-globe thermometer method a feasible course of action?, in: 2018 IEEE International Conference On Environment And Electrical Engineering And 2018 IEEE Industrial And Commercial Power Systems Europe (EEEIC/I CPS Europe), 2018, pp. 1–7, https://doi.org/10.1109/EEEIC.2018.8493714.

[38] Z. Tan, K.K.-L. Lau, E. Ng, Planning strategies for roadside tree planting and outdoor comfort enhancement in subtropical high-density urban areas, Build. Environ. 120 (2017) 93–109, https://doi.org/10.1016/j.buildenv.2017.05.017.